Phase space reconstruction using input-output time series data

David M. Walker[1,2] and Nicholas B. Tufillaro[2,1]
[1]*Department of Applied Science, College of William and Mary, Williamsburg, Virginia 23187-8795*
[2]*HP Laboratories, MS4-AD, 1501 Page Mill Road, Palo Alto, California 94304-1126*
(Received 12 April 1999)

In this paper we suggest that an extension of a procedure recently proposed by Wayland *et al.* [Phys. Rev. Lett. **70**, 580 (1993)] for recognizing determinism in an autonomous time series can also be used as a diagnostic for determining an appropriate embedding dimension for driven (''input-output'') systems. We compare the results of this extension to the results produced by the extensions to the method of false nearest neighbors put forward by Rhodes and Morari [*Proceedings of the American Control Conference, Seattle*, edited by The American Automatic Control Council (IEEE, Piscataway, 1995)] and the method of averaged false nearest neighbors by Cao *et al.* [Int. J. Bifurcation Chaos **8**, 1491 (1998)]. [S1063-651X(99)12510-8]

PACS number(s): 05.45.−a

I. INTRODUCTION

In this paper we suggest that an extension of a procedure recently proposed by Wayland *et al.* [1] for recognizing determinism in an autonomous time series can also be used as a diagnostic for determining an appropriate embedding dimension for driven (''input-output'') systems. We compare the results of this new diagnostic with the results of two other diagnostics recently proposed in the literature [2,3].

The paper by Casdagli [4] is a common starting point for many researchers when faced with the problem of applying nonlinear dynamics techniques to the modeling of systems using input-output time series data. The main idea drawn from this paper is that an extended phase space can be reconstructed from the input and output time series. If we denote the output time series by $y(t)$ and the input time series by $u(t)$ then an extended reconstructed phase space for nonautonomous systems can be formed with vectors

$$z(t)=[y(t-(k-1)s),\ldots,y(t-s),y(t),$$

$$u(t-(l-1)s),\ldots,u(t-s),u(t)], \qquad (1)$$

where k is the embedding dimension of the output time series and l is the embedding dimension of the input time series. We have assumed that the time delay s is the same for the input and the output time series although this need not be the case. In the following we assume that an appropriate time delay has been found. An appropriate value for the time delay can be found using methods such as autocorrelation [5] or mutual information [6]. In addition we will normalize all time series (to lie in the range -2 and 2) for reasons to be discussed later.

For a given time delay the problem is to design a diagnostic to find appropriate values for k and l from time series data. Rhodes and Morari [2] have extended the false nearest neighbor algorithm of Kennel *et al.* [7] to determine k and l. More recently Cao *et al.* [3] have suggested an alternative method by extending the work of [9]. The work of [9] is in itself an extension of the false nearest neighbor method called averaged false nearest neighbors. In this paper we argue that the method of Wayland *et al.* [1] can similary be extended to provide such a diagnostic.

The outline of this paper is as follows: In the next section we describe the Wayland method for detecting determinism in a time series, and explain why it can be used as a diagnostic for determining an appropriate embedding dimension for phase space reconstruction. We reinforce our contention with an example using data from the chaotic Lorenz system. We then introduce our scheme for reconstruction using input-output time series data by extending the Wayland method. To illustrate our technique we apply it to data from Duffing's equation and to data obtained from a model of a bipolar junction transistor (BJT). We compare our results with those obtained from an implementation of the methods of [2] and [3].

II. WAYLAND METHOD

According to Wayland *et al.* [1] a time series is said to be deterministic if the reconstructed vectors

$$x(t)=[y(t-(k-1)s),\ldots,y(t-s),y(t)]$$

can be modeled as the iteration of a continuous function f. A test for continuity can be developed based on the fact that points close together will map to points close together under a single iteration of the map f.

Let x_0 be a reference vector chosen from $x(t), t=1,2,\ldots,N$, and let $x_1,x_2,\ldots,x_m$ be the m nearest neighbors of x_0 chosen from $x(t), t=1,2,\ldots,N$. In addition, we ensure that none of these points are (strongly) temporally correlated. Let $y_0,y_1,\ldots,y_m$ be the images of the vector x_0 and its neighbors respectively. If the data is deterministic *and* correctly embedded we expect the translation vectors

$$v_j=y_j-x_j$$

to be nearly equal provided the near neighbors are within a small region of phase space. Wayland *et al.* quantify this insight by computing the translation error

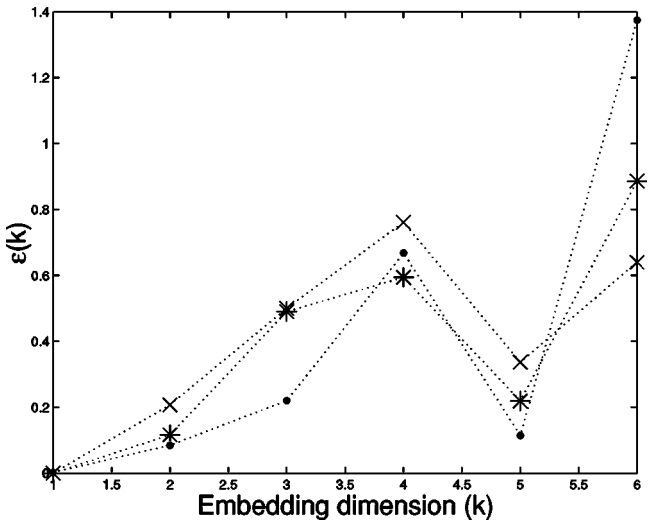

FIG. 1. Plot of $\epsilon(k)$ for various numbers of near neighbors, $\bullet - m=5$, $* - m=10$, and $x - m=20$. We notice that a maximum of $\epsilon(k)$ occurs at $k=4$ for all curves. We thus conclude that $k=4$ is a suitable embedding dimension, which is consistent with known results.

$$E_{trans}=\frac{1}{m+1}\sum_{j=0}^{m}\frac{\|v_j-\langle v\rangle\|^2}{\|\langle v\rangle\|^2},$$

where

$$\langle v\rangle=\frac{1}{m+1}\sum_{j=0}^{m}v_j.$$

This local translation error is extended to a more global measure of translation error by choosing N_r random reference vectors from $x(t), t=1,2,\ldots,N$. For each reference vector we compute an associated E_{trans} and then calculate the global translation error $E=\text{median}(E_{trans})$.

In addition to the embedding dimension k and the time delay s there are two other free parameters. These are N_r the number of reference vectors and m the number of near neighbors. We will remove the parameter N_r by using all embedded data points as reference vectors just like the extensions in [2] and [3]. In so doing we will take E to be the average of E_{trans} rather than the median. E is thus a function of embedding dimension. Following Cao [9] we will calculate the quantity

$$\epsilon(k)=\frac{E(k+1)}{E(k)}.$$

The translation error $E(k)$ will generally decrease with increasing embedding dimension. As k increases $\epsilon(k)$ will typically rise; however, there will be a marked change (a decrease) in the slope of $\epsilon(k)$ when a suitable embedding dimension is attained. This change is distinctive and the k at which it occurs is what we will choose as the embedding dimension. There is even the possibility of an increase in $E(k)$ for large k due to decorrelations in the embedded data. In this case $\epsilon(k)$ will begin to decrease and the decrease in slope will correspond to a local maximum of $\epsilon(k)$. We will study how robust this prescription is to the observational noise level in the data and the number m of neighbors chosen in the calculations.

III. INPUT-OUTPUT DIAGNOSTIC

The above diagnostic can be extended to input-output time series data in a simple manner. The scheme is essentially the same but the method of determining nearest neighbors is modified. The nearest neighbors of a vector x_0 are instead determined in the extended reconstructed space from the vectors $z(t)$ [see Eq. (1)]. The vector x_0 is associated with a vector z_0. Let $z_1, z_2, \ldots, z_m$ be the (decorrelated) nearest neighbors of z_0. We denote by w_j the images of these near neighbors. For each $z_j, j=1,2,\ldots,m$ we project down to the ''x'' subspace, i.e., $x_j=Cz_j$ and $y_j=Cw_j$ where C picks out the parts of $z(t)$ constructed using the output time series. We calculate the translation error as before with these vectors.

We note that the inputs can possibly be deterministic or stochastic. For deterministic inputs continuity in input-output space can be assured by an application of Taken's theorem to this extended phase space. The case of stochastic forcing is more subtle but results of Stark *et al.* [8] can be applied. A simple minded explanation of the scheme is based on the fact that vectors close in reconstructed phase space subject to similar inputs should end up in the same place.

The choice of the near neighbors in this extended reconstructed space may be dominated by closeness in reconstructed phase space or closeness in the reconstructed input phase space. For example two vectors may be deemed close in the extended phase space because their distance apart in phase space masks the difference in the inputs. The two vectors although close in phase space could be subjected to vastly different inputs thus compromising the translation errors. To avoid this eventuality we suggest normalizing the output and input time series.

Once again following the paper of Cao *et al.* [3] we calculate

$$\epsilon(k,l)=\frac{E(k+1,l)}{E(k,l)}.$$

To distinguish between different values of l we choose the $\epsilon(k,l)$ for which $k+l$ is a minimum. We also favor values of k and l where $l>k$. For example if $\epsilon(k,l)$ suggests two choices $(k,l)=(2,2)$ and $(k,l)=(1,3)$ say, we will choose the latter. A reason for this choice comes from our interest in modeling electronic device components [10] for the purpose of simulations. We believe a model with as little feedback as possible, i.e., small k, should be more stable under iteration than a model with large k.

IV. EXAMPLES

We present an example illustrating the effectiveness of the method when applied to output time series data. The output data is obtained by integrating the chaotic Lorenz equations. For this example appropriate embedding dimensions are known from studies elsewhere (see for example Abarbanel *et al.* [11]). We study how robust our prescription

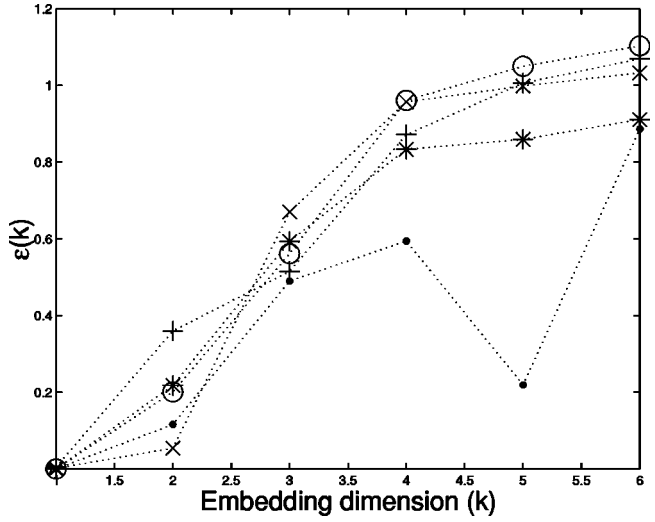

FIG. 2. Plot of $\epsilon(k)$ with $m=10$ for data sets corrupted with observational noise. $\bullet=0\%$, $*=5\%$, $x=10\%$, $o=20\%$ and $+=40\%$. We see that the decrease in the slope of $\epsilon(k)$ at $k=4$ persists for noise levels upto 10% but then degrades thereafter.

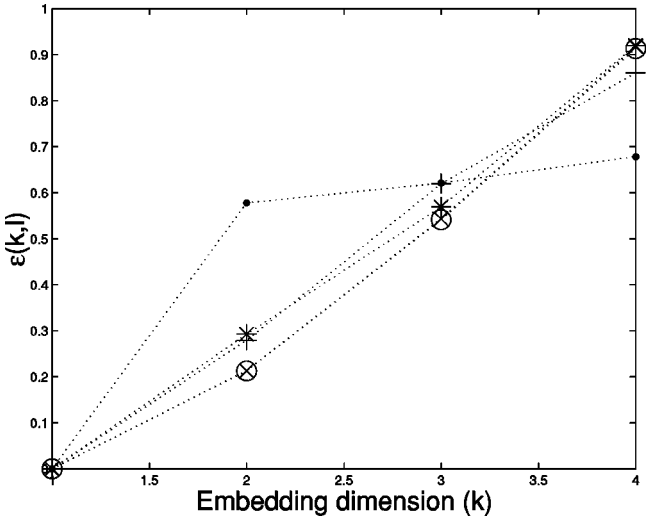

FIG. 3. Plot of $\epsilon(k,l)$ for $l=1,\ldots,5$. $\bullet$-$l=1$, $*$–$l=2$, x–$l=3$, o–$l=4$, and $+$–$l=5$. We see that choosing $k=2$ and $l=1$ is a suitable and minimal choice for embedding the Duffing input-output time series data.

is to observational noise in the data and the number of near neighbors in the diagnostic.

We present two examples to illustrate the effectiveness of our extension to the Wayland scheme to accomodate input-output time series data. In the first example we consider data from Duffing's equation. Once again we study the robustness of our method to observational noise on the input and output time series, and the number of near neighbors on the diagnostic. We also compare the results of our method to the results produced by using the methods suggested by Rhodes and Morari [2] and Cao *et al.* [3]. The second data set we study using our method is obtained from simulating a model of a bipolar junction transistor (BJT), the Ebers-Moll model [12].

A. Output time series

The Lorenz differential equations are

$$\dot{u}=\sigma(-u+v),$$

$$\dot{v}=ru-v-uw,$$

$$\dot{w}=-bw+uv,$$

where for $\sigma=10$, $r=28$ and $b=\frac{8}{3}$ chaotic solutions are generated. We generate time series data by integrating the Lorenz equations using a variable step-size Runge-Kutta method: matlab's `ode23` routine, and output the u coordinate every 0.01 time units after transients have diminished. (That is, we integrate long enough for the dynamics to evolve on the attractor.) We obtain a 10 000 point time series, and determine a lag $s=35$ by choosing the first minimum of the average mutual information function [6].

We apply the Wayland *et al.* diagnostic for different numbers of neighbors $m=5$, 10, and 20 and with a decorrelation interval of 10. The results are shown in Fig. 1. We see that at an embedding dimension of 4 the slope of $\epsilon(k)$ decreases and for all curves we actually obtain a local maximum. Thus, an embedding dimension of 4 is suggested consistent with known values. We also notice that this value appears to persist with respect to the number of near neighbors used in the diagnostic. We have obtained similar results for even higher numbers of nearest neighbors, and so to reduce the number of figures we shall henceforth present only the results for $m=10$.

To see how robust the diagnostic is to noise in the data we add observational noise at various levels. The noise added is zero mean Gaussian with standard deviations of 5%,10%, 20%,and 40% the standard deviation of the clean Lorenz signal. In Fig. 2 we show how $\epsilon(k)$ varies for $m=10$ on each of the noisy data sets. As the noise level in the data increases we no longer see a local maximum at $k=4$. All curves, however, show a decrease in their slopes at an embedding dimesion of 4 although there is a graceful

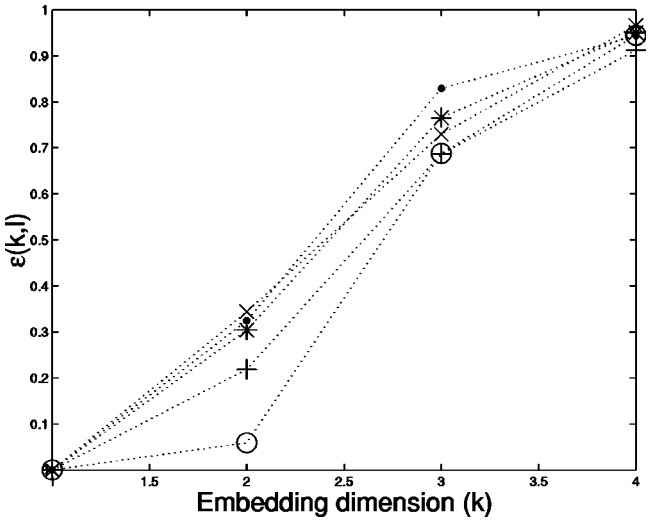

FIG. 4. Plot of $\epsilon(k,l)$ for $l=1,\ldots,5$. $\bullet$–$l=1$, $*$–$l=2$, x–$l=3$, o–$l=4$, and $+$–$l=5$. We see that the effect of the noise has been to increase the dimension suggested by the diagnostic. Examining the figure we see that the embedding strategy $(k,l)=(3,1)$ is suggested.

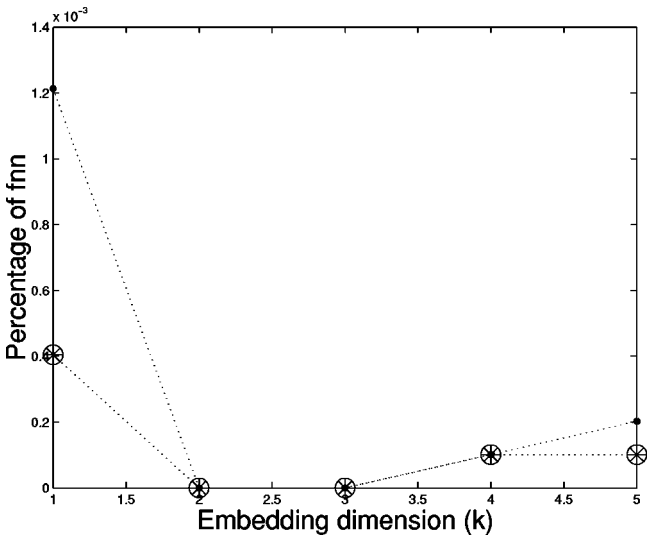

FIG. 5. Plot of the percentage of false nearest neighbors for $l=1,\ldots,5$. $\bullet$–$l=1$, $*$–$l=2$, x–$l=3$, o–$l=4$, and $+$–$l=5$. We see that consistent with our diagnostic the method suggests embedding with $(k,l)=(2,1)$.

dropoff in performance for noise levels above 10%. Thus, despite the dropoff in performance the diagnostic appears to be robust against the effects of high levels of noise.

B. Input-output time series

The first example we use to study our method is Duffing's differential equation. This equation is given by

$$\dot{u}=v,$$

$$\dot{v}=u-u^3-\epsilon v+\gamma\cos(\omega t).$$

We use parameter values that generate chaotic solutions, i.e., $\epsilon=0.25$, $\gamma=0.3$, and $\omega=1.0$. We consider the system as a driven system with the input $g(t)=\cos(\omega t)$. We generate a

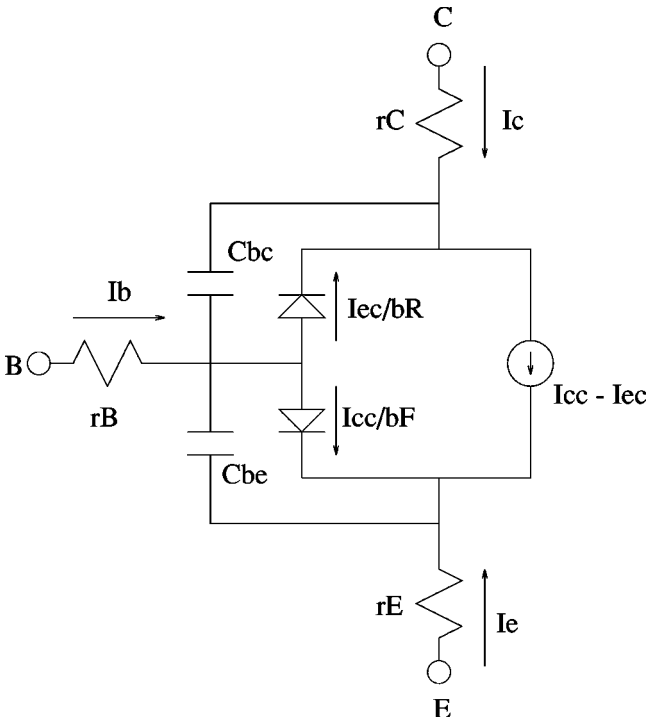

FIG. 7. Ebers-Moll transistor model.

10 000 point output time series by integrating the differential equations and outputing the u component every 0.05 time units after transients have diminished. The input time series is obtained by evaluating $g(t)$ every 0.05 time unit. We use a lag of $s=26$ by locating the first minimum of the average mutual information function applied to the output time series.

In Fig. 3 we show the result of applying our diagnostic with $m=10$ to clean input and output data. We see that for the case $l=1$, i.e., embedding using one input, there is a marked decrease in the slope of $\epsilon(k,l)$ at $k=2$. Since all other curves do not show this decrease our diagnostic sug-

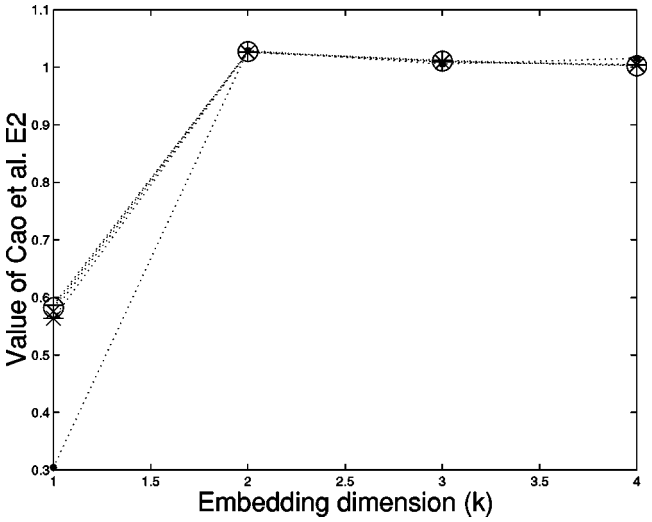

FIG. 6. Plot of Cao *et al.* $E2$ statistic for $l=1,\ldots,5$. $\bullet$–$l=1$, $*$–$l=2$, x–$l=3$, o–$l=4$, and $+$–$l=5$. We see that consistent with our diagnostic this method suggests embedding with $(k,l)=(2,1)$.

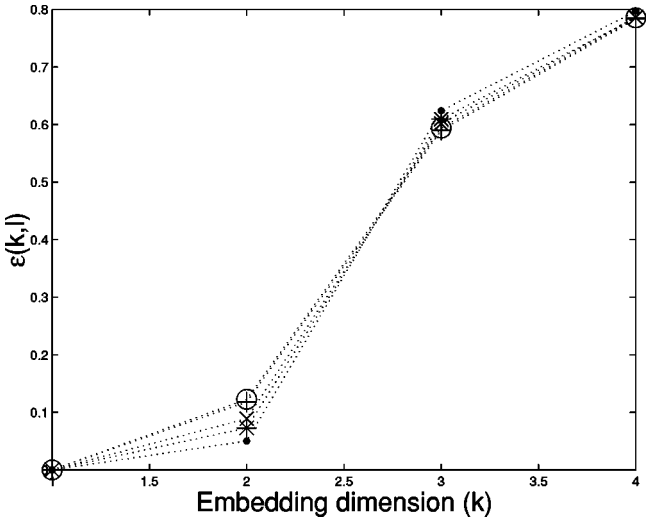

FIG. 8. Plot of $\epsilon(k,l)$ for $l=1,\ldots,5$. $\bullet$–$l=1$, $*$–$l=2$, x–$l=3$, o–$l=4$, and $+$–$l=5$. We see that choosing $k=3$ and $l=1$ is a suitable and minimal choice for embedding the BJT input-output time series data.

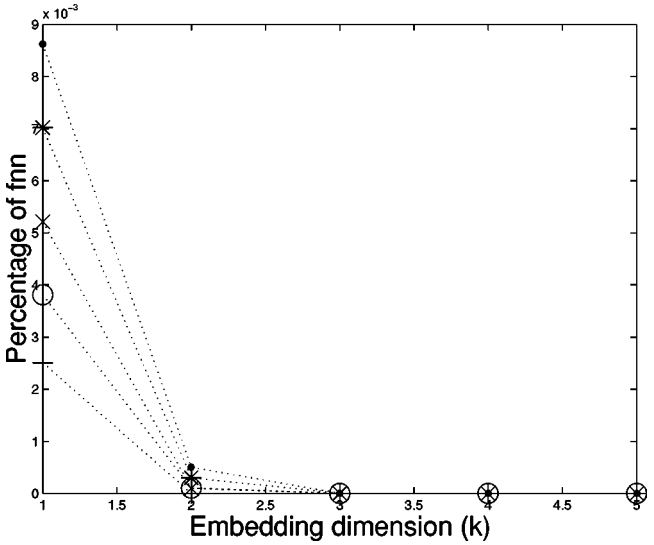

FIG. 9. Plot of the percentage of false nearest neighbors for $l=1,\ldots,5$. ●$-l=1$, *$-l=2$, $x-l=3$, $o-l=4$, and $+-l=5$. We see that consistent with our diagnostic the method suggests embedding with $(k,l)=(3,1)$.

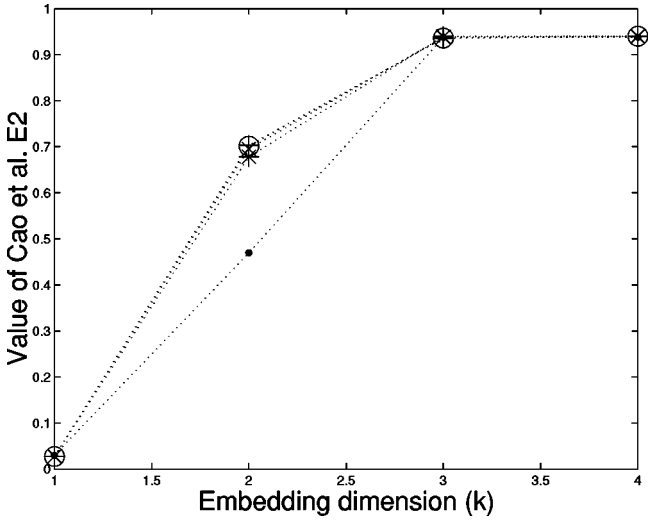

FIG. 10. Plot of Cao *et al.* $E2$ statistic for $l=1,\ldots,5$. ●$-l=1$, *$-l=2$, $x-l=3$, $o-l=4$, and $+-l=5$. We see that consistent with our diagnostic this method suggests embedding with $(k,l)=(3,1)$.

gests embedding the output data in two dimensions ($k=2$) and using one input ($l=1$). To see how this answer persists in the presence of noise we show in Fig. 4 the results of applying our diagnostic with $m=10$ to data corrupted with 10% observational noise at *both* the inputs and outputs. In this case we notice that the effect of the noise has caused the suggested embedding dimension to increase, but even with such noisy data it was still possible to detect a suitable embedding dimension. All curves show a marked decrease in the slope of $\epsilon(k,l)$ at $k=3$. Since we favor embedding parameters with as small a value of $k+l$ as possible, our diagnostic suggests embedding using $k=3$ and $l=1$.

For comparison we show in Figs. 5 and 6 the results of applying the Rhodes and Morari scheme and the Cao *et al.* scheme to the clean data respectively. In the Rhodes and Morari scheme the values of k (and l) for which the percentage of false nearest neighbors drops to zero, or plateau's at a noise floor, are taken as the embedding parameters. The embedding parameters suggested by the Cao *et al.* scheme are those for which the curves plateau at $E2=1$. We see that both schemes suggest embedding with $(k,l)=(2,1)$, which is consistent with the values suggested by our diagnostic.

The second example we study to compare our method uses input-ouput data obtained from a nonlinear transistor. We consider the Ebers-Moll model [12] for a BJT shown schematically in Fig. 7. We obtain time series data by applying voltages across the base and emitter, and across the collector and emitter. We integrate the circuit equations and obtain the currents at I_c and I_b. For the purposes of this study we will consider the current I_c as the output data and the voltage across the collector and emitter, V_{ce} as the input data.

We integrate from time zero to time $1e-6$ outputing every $1e-10$ steps. This generates approximately 10 000 input-output data points. The voltage V_{be} consists of a fixed dc-offset plus an amplitude modulated signal given by $[1+m\sin(\omega_m t)]V_c\sin(\omega_c t)$, where $m=4/5$, $V_c=5V$, $\omega_m=50$ MHz and $\omega_c=5$ GHz. The voltage V_{ce} (our input sequence) consists of a fixed dc-offset and a one-tone signal $f=20\sin(50\pi t/T)$, where $T=1e-6s$.

In Fig. 8 we show the results of applying our diagnostic with $m=10$. (We used a lag of 5 obtained by locating the first minimum of the average mutual function applied to the output data.) Studying the figure we see that the slope of all curves of $\epsilon(k,l)$ begins to decrease at $k=3$. Once again since we favor using a smallest total embedding dimension as possible, a suitable embedding strategy is to choose $k=3$ and $l=1$. In Figs. 9 and 10 we show the results obtained by using the diagnostics of Rhodes and Morari and Cao *et al.* We see that the embedding strategies suggested by these two diagnostics are consistent with the results we obtained with our method.

V. CONCLUSION

We have demonstrated that an extension of a procedure originally proposed by Wayland *et al.* to recognize determinism in an autonomous time series can also be used as a diagnostic for determining an appropriate embedding dimension for a driven (''input-output'') system. We have shown that the diagnostic is robust to the effects of noise and produces results consistent with those of other diagnostics.

ACKNOWLEDGMENTS

We thank Paul Gross for deriving the circuit equations for the BJT transistor. This work was supported in part by the NSF through Grant No. 9724707. We thank Hewlett-Packard for their hospitality during recent visits.

[1] R. Wayland, D. Bromley, D. Pickett, and A. Passamente, Phys. Rev. Lett. **70**, 580 (1993).

[2] C. Rhodes and M. Morari, in *Proceedings of the American Control Conference, Seattle*, edited by The American Automatic Control Council (IEEE, Piscataway, 1995), pp. 2190–2195.

[3] L. Cao, A. Mees, K. Judd, and G. Froyland, Int. J. Bifurcation Chaos Appl. Sci. Eng. **8**, 1491 (1998).

[4] M. Casdagli, in *Nonlinear Modeling and Forecasting, SFI Studies in the Sciences of Complexity*, edited by M. Casdagli and S. Eubank (Addison-Wesley, Reading, MA, 1992), pp. 265–281.

[5] H. Kantz and T. Schrieber, *Nonlinear Time Series Analysis* (Cambridge University Press, Cambridge, England, 1997).

[6] A. M. Fraser and H. L. Swinney, Phys. Rev. A **33**, 1134 (1986).

[7] M. B. Kennel, R. Brown, and H. D. I. Abarbanel, Phys. Rev. A **45**, 3403 (1992).

[8] J. Stark, D. S. Broomhead, M. E. Davis, and J. Huke, Nonlinear Analysis **30**, 5303 (1997).

[9] L. Cao, Physica D **110**, 43 (1997).

[10] D. M. Walker, R. Brown, and N. B. Tufillaro, Phys. Lett. A **255**, 236 (1999).

[11] H. D. I. Abarbanel, R. Brown, J. J. Sidorowich, and L. S. Tsimring, Rev. Mod. Phys. **65**, 1331 (1993).

[12] I. Getreu, *Modeling the Bipolar Transistor* (Tektronix Inc, Oregon, 1967).